J. Opt. B: Quantum Semiclass. Opt. **2** (2000) 510–516. Printed in the UK PII: S1464-4266(00)13124-6

Temporal heterodyne detector for multitemporal mode quantum state measurement

C Iaconis, E Mukamel and I A Walmsley

The Institute of Optics, University of Rochester, Rochester, NY 14627, USA

Received 7 April 2000

Abstract. We propose a novel method for measuring the multitemporal mode quantum state of repetitive radiation fields with ultrafast temporal resolution. The technique incorporates spectrometers at the output ports of a DC-balanced four-port apparatus. The signal field to be measured is delayed in time with respect to an ultrashort local oscillator pulse which is taken to be in a large-amplitude single temporal mode coherent state. A quantum-mechanical analysis shows that the Fourier transform of the spectrally resolved difference counts is proportional to the multitemporal mode Q-function describing the signal field statistics. We apply the technique to reconstruct the multitemporal mode Q-function from simulated data of repetitive broadband chaotic light from which we calculate the photon number correlations between pairs of temporal modes.

Keywords: Heterodyne detection, quantum measurement, quantum state reconstruction, ultrafast optics, multimode coherence

1. Introduction

The aim of quantum field characterization is to reconstruct from experimentally accessible data the quantum state of the optical field. Specifically, this means reconstructing a representation of the density operator of the field from a set of probability distributions of a tomographically complete set of observables. The DC-balanced homodyne detector [1, 2] has gained widespread acceptance as the key tool for such measurements. Such a detector measures the amplitude fluctuations for a single quadrature of the signal field. By a suitable arrangement of two balanced homodyne detectors, Walker and Carroll [3] devised a scheme to measure simultaneously both the in-phase and in-quadrature components of a single-mode field. This eight-port arrangement therefore measures a representation of the density matrix in the space of the two quadrature field amplitudes; in particular, it measures the Q-function, a positive-definite phase-space quasiprobability distribution [4]. A more recent technique measures the statistics of a set of rotated quadrature amplitudes using a typical four-port arrangement, by adjusting the phase of the local oscillator (LO). From the data set it is possible to reconstruct the Wigner quasiprobability distribution of the light field by means of the inverse Radon transform [5, 6]. For this reason the technique is known as optical homodyne tomography (OHT). Alternatively, the quantum state of the light field can be reconstructed from the tomographic data set by using a direct sampling method in which the density matrix in the photon number basis is reconstructed by averaging a sample function [7–9].

Using a strong classical ultrashort pulsed field as the LO, OHT permits the statistical characterization of repetitive weak optical fields on ultrafast timescales [10, 11]. Although an emphasis has been placed on measuring the statistics of a single temporal slice (or mode) of the optical field, there has been an increased effort directed toward multitemporal mode characterization, which is essential for situations in which the temporal modes are correlated at the quantum level. Recent proposals suggest the use of a LO consisting of two ultrashort pulses with adjustable relative phase and independently controlled amplitudes for measuring the quantum statistics of two temporal modes simultaneously [12, 13]. Phase-independent coherences, such as two-time photon number correlations [14], have been measured in experiments using such configurations. More recently, the reconstruction of the two-mode joint photon statistics of squeezed light from a parametric amplifier has been demonstrated [15]. In addition, there have been several proposals for more generalized schemes for two-mode [16] (and even multi-mode [17]) state measurement using generalized phase-space manipulations, and experiments directed toward reconstruction of the density operator itself are in progress. Nonetheless, however it is undertaken, complete characterization of the repetitive quantum field requires the measurement of the quantum statistics for all of the temporal modes simultaneously.

An alternative class of measurement devices, based on heterodyne detection, allows for the measurement of any one of an arbitrary number of modes. Such methods have been applied to the problem of measuring the spectral and spatial modes of quantum fields. For instance, a heterodyne method for measuring the quantum statistics

1464-4266/00/040510+07$30.00

of a signal occupying a plane-wave mode (characterized by its propagation vector) was proposed by Raymer *et al* [18]. In their device the signal and LO are interfered at a beamsplitter. Since they are non-collinear, the signal and LO have different propagation vectors and consequently occupy different plane-wave modes. The resulting interference beating at the output ports of the beamsplitter is spatially resolved by detector arrays. Since each plane-wave mode beats with the LO at a distinct spatial frequency, the data are easily filtered to pick out the beat note and corresponding mode of interest. This is precisely the approach adopted in conventional spectral heterodyne detection [19], in which the signal and LO fields occupy different optical frequency modes. In this case, the data are recorded as a function of time, and the period of the temporal beating is determined by the optical frequency difference, known as the intermediate frequency, between the LO and the signal mode of interest. Although heterodyne techniques have been applied to the problem of measuring the quantum statistics of a field occupying any one of a number of spatial or spectral modes, to our knowledge they have not been applied to the problem of measuring the quantum statistics of a signal occupying multiple temporal modes.

In this paper, we propose a time domain analogue of the conventional spectral and spatial heterodyne detection techniques, and show that such a device does, in fact, simultaneously measure the multimode statistics of repetitive quantum fields that occupy an arbitrary number of temporal modes. Because of the similarity of our method to conventional heterodyne methods, we generically refer to the technique as multimode temporal heterodyne detection (MTHD). Section 2 of this paper describes the apparatus and data inversion procedure. Section 3 presents a quantum analysis of the technique that shows explicitly that the device measures the multitemporal mode Q-function describing the signal field statistics. Section 4 applies the inversion routine to simulated MTHD data of repetitive thermal-like light, and shows that a minimal number of shots (realizations of the ensemble) are required to reconstruct the two-time photon number correlation of the signal field from the measurement.

2. Multimode temporal heterodyne detector

Figure 1 is a schematic of the MTHD apparatus. A short pulse LO and a signal field (s) impinge on the two input ports of a broadband 50 : 50 beamsplitter. The strong LO occupies a single time slice (or temporal mode) at time zero. The weak signal field is delayed in time with respect to the LO ($t > 0$), and may occupy multiple temporal modes. The temporal modes preceding the LO ($t < 0$) are occupied by the vacuum. Since the LO and signal fields are delayed with respect to one another in time, the combined fields beat in frequency. The spectral beating at the two output ports of the beamsplitter (designated (a) and (b)) is resolved by a pair of spectrometers and recorded by a pair of linear detector arrays. Each detector array consists of N pixels indexed by the subscript j, which runs from $-(N-1)/2$ to $(N-1)/2$. The spatial width of each detector element corresponds to a spectral width $\delta\nu$ such that the mean frequency incident on the jth detector element is $\nu_j = \delta\nu \times j$, referenced to an optical carrier frequency ω_0. The jth detector element of each array records the incident number of photons, n_j, within the frequency range $\nu_j \pm \delta\nu/2$.

Every input signal pulse is an individual realization of the ensemble. The procedure for reconstructing the quantum statistics of this ensemble is as follows: on each shot, the number of photons incident on the detector arrays, $\{n_j^{(a)}\}$ and $\{n_j^{(b)}\}$, is recorded, and the set of difference photon numbers, $\{\Delta_j\}$, where

$$\Delta_j = n_j^{(a)} - n_j^{(b)} \tag{1}$$

is evaluated by a multichannel differencer. Next, the discrete Fourier transform of the set of difference photon numbers is calculated,

$$\kappa_k = \sum_j \Delta_j \mathrm{e}^{-\mathrm{i}2\pi jk/N}, \tag{2}$$

which returns the set of complex numbers $\{\kappa_k\}$. The time index k ranges from $-(N-1)$ to $(N-1)$. The corresponding temporal step size is $(\delta\nu \times N)^{-1}$. That is, $t_k = k/(\delta\nu \times N)$. The difference photon numbers are real and consequently $\kappa_{-k} = \kappa_k^*$. Moreover, time index $k = 0$ corresponds to the LO mode alone. Therefore, only the subset of $\{\kappa_k\}$ for $1 \leqslant k \leqslant (N-1)$ is of interest.

The sets of photon numbers $\{n_j^{(a)}\}$ and $\{n_j^{(b)}\}$ are recorded, the set of difference photon numbers, $\{\Delta_j\}$, is evaluated, and the discrete Fourier transform, κ_k, is calculated for a sufficient number of realizations of the ensemble that the $(N-1)$ complex variable probability distribution, $P_\kappa(\{\kappa_k\})$, for obtaining the set of complex numbers $\{\kappa_k\}$ is constructed with adequate dynamic range. $P_\kappa(\{\kappa_k\})$ is directly related to the probability distribution, $P_\Delta(\{\Delta_j\})$, for measuring the joint set of difference counts $\{\Delta_j\}$. The relation is readily established by comparing their characteristic functions, $C_\kappa(\{\xi_k\})$ and $C_\Delta(\{\gamma_j\})$,

$$\begin{aligned} C_\kappa(\{\xi_k\}) &= \left\langle \exp\left[-\mathrm{i}\sum_k (\xi_k\kappa_k + \xi_k^*\kappa_k^*)\right]\right\rangle_c \\ &= \int \mathrm{d}^2\{\kappa_k\} P_\kappa(\{\kappa_k\}) \exp\left[-\mathrm{i}\sum_k (\xi_k\kappa_k + \xi_k^*\kappa_k^*)\right], \end{aligned} \tag{3}$$

and

$$\begin{aligned} C_\Delta(\{\gamma_j\}) &= \left\langle \exp\left[-\mathrm{i}\sum_j \gamma_j\Delta_j\right]\right\rangle_c \\ &= \int \mathrm{d}\{\Delta_j\} P_\Delta(\{\Delta_j\}) \exp\left[-\mathrm{i}\sum_j \gamma_j\Delta_j\right]. \end{aligned} \tag{4}$$

The angled brackets labelled by the subscript c indicate a classical ensemble average. Comparing equations (3) and (4) and recalling that κ_k is related to the difference photon numbers Δ_j by the Fourier transform of equation (2), we recognize that the characteristic functions are simply related by

$$\begin{aligned} C_\kappa(\{\xi_k\}) = C_\Delta\Bigg(\Bigg\{\gamma_j = \sum_k \Bigg(\xi_k \exp\left[\frac{-\mathrm{i}2\pi jk}{N}\right] \\ + \xi_k^* \exp\left[\frac{\mathrm{i}2\pi jk}{N}\right]\Bigg)\Bigg\}\Bigg). \end{aligned} \tag{5}$$

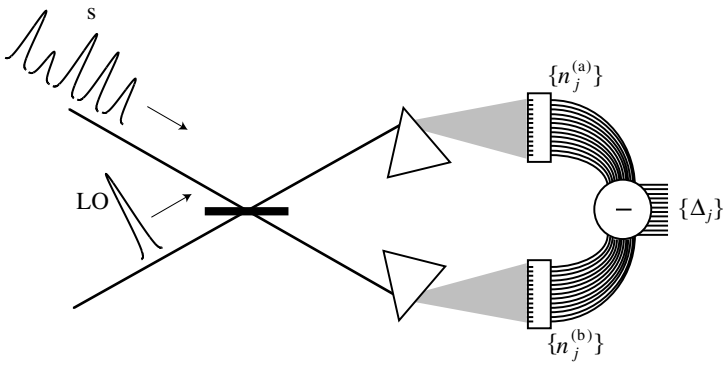

Figure 1. The proposed MTHD apparatus. A strong, single temporal-mode LO and a weak, multitemporal mode signal (s) impinge on the two input ports of a beamsplitter. The signal is delayed in time with respect to the LO and consequently the combined fields beat in frequency. The beating at the two output ports of the beamsplitter (designated (a) and (b)) is resolved by a pair of spectrometers, and the number of photons per spectral mode, $\{n_j^{(a)}\}$ and $\{n_j^{(b)}\}$, is recorded by a pair of linear detectors, indexed by the subscript j. A multichannel differencer evaluates the set of difference numbers, $\{\Delta_j\}$.

The following section applies photodetection theory to evaluate the characteristic function, $C_\Delta(\{\gamma_j\})$, and then uses the relation of equation (5) to show that $P_\kappa(\{\kappa_k\})$ is, in fact, proportional to the multitemporal mode Q-function describing the quantum state of the signal field.

3. Quantum analysis of the MTHD technique

The proposed apparatus builds up, in a shot-to-shot fashion, the probability distribution, $P_\kappa(\{\kappa_k\})$, for obtaining the set of Fourier transformed difference photon numbers, $\{\kappa_k\}$, where $1 \leqslant k \leqslant (N-1)$. In this section we derive, through the application of photodetection theory, an explicit relation between $P_\kappa(\{\kappa_k\})$ and the multitemporal mode Q-function, $Q(\{\beta_k\})$, which describes the joint quantum statistic of the multitemporal mode signal field. The strategy for relating $P_\kappa(\{\kappa_k\})$ to $Q(\{\beta_k\})$ is as follows: first, we apply photodetection theory to evaluate the characteristic function, $C_\Delta(\{\gamma_j\})$, associated with $P_\Delta(\{\Delta_j\})$. Then, using the relation established in equation (5), we reconstruct $C_\kappa(\{\xi_k\})$ from $C_\Delta(\{\gamma_j\})$. Finally, we compare $C_\kappa(\{\xi_k\})$ with the characteristic function associated with $Q(\{\beta_k\})$.

From photodetection theory it is known [20] that $C_\Delta(\{\gamma_j\})$ is related to the characteristic function, $C_{n^{(a)}n^{(b)}}(\{\mu_j^{(a)}, \mu_j^{(b)}\})$, associated with the joint measurement of the set of photon numbers $\{n_j^{(a)}\}$ and $\{n_j^{(b)}\}$ recorded by the detector arrays,

$$C_\Delta(\{\gamma_j\}) = C_{n^{(a)}n^{(b)}}(\{\mu_j^{(a)} = \gamma_j, \mu_j^{(b)} = -\gamma_j\}) \qquad (6)$$

where

$$C_{n^{(a)}n^{(b)}}(\{\mu_j^{(a)}, \mu_j^{(b)}\}) = \left\langle : \exp\left[\sum_j (\exp[-\mathrm{i}\mu_j^{(a)}] - 1)\hat{n}_j^{(a)} + \sum_j (\exp[-\mathrm{i}\mu_j^{(b)}] - 1)\hat{n}_j^{(b)} \right] : \right\rangle. \qquad (7)$$

The :: notation has the customary meaning that the operators within the symbol should be arranged in normal order. By combining equations (6) and (7) we express $C_\Delta(\{\gamma_j\})$ in terms of the output port spectral mode photon number operators $\hat{n}_j^{(a)}$ and $\hat{n}_j^{(b)}$,

$$C_\Delta(\{\gamma_j\}) = \left\langle : \exp\left[\sum_j (\exp[-\mathrm{i}\gamma_j] - 1)\hat{n}_j^{(a)} + \sum_j (\exp[\mathrm{i}\gamma_j] - 1)\hat{n}_j^{(b)} \right] : \right\rangle. \qquad (8)$$

To evaluate $C_\Delta(\{\gamma_j\})$ we must calculate the quantum ensemble average of equation (8). This task may be simplified by defining the scaled difference counts $\bar{\Delta}_j = \Delta_j/|\varepsilon|$, where ε is the complex amplitude of the LO, and to work with the scaled difference count probability distribution $P_{\bar{\Delta}}(\{\bar{\Delta}_j\})$ [21]. The associated characteristic function is related to $C_\Delta(\{\gamma_j\})$ by

$$C_{\bar{\Delta}}(\{\gamma_j\}) = (|\varepsilon|)^{-N} C_\Delta(\{\gamma_j/|\varepsilon|\}). \qquad (9)$$

With the aid of equation (8), we rewrite $C_{\bar{\Delta}}(\{\gamma_j\})$ in terms of the output port spectral mode photon number operators,

$$C_{\bar{\Delta}}(\{\gamma_j\}) = (|\varepsilon|)^{-N}\left\langle : \exp\left[\sum_j \left(\exp\left[\frac{-\mathrm{i}\gamma_j}{|\varepsilon|}\right] - 1\right)\hat{n}_j^{(a)} + \sum_j \left(\exp\left[\frac{\mathrm{i}\gamma_j}{|\varepsilon|}\right] - 1\right)\hat{n}_j^{(b)} \right] : \right\rangle. \qquad (10)$$

To further simplify the evaluation, we follow [20] and [21] and Taylor-expand the exponentials of the form $\exp[\pm\mathrm{i}\gamma_j/|\varepsilon|]$ in the expression for $C_{\bar{\Delta}}(\{\gamma_j\})$, omitting terms of higher than second order since $\gamma_j/|\varepsilon| \ll 1$ for large $|\varepsilon|$. Then, the scaled difference count characteristic function simplifies to

$$C_{\bar{\Delta}}(\{\gamma_j\}) = (|\varepsilon|)^{-N} \times \left\langle : \exp\left[\frac{-\mathrm{i}}{|\varepsilon|} \sum_j \gamma_j \hat{\Delta}_j - \sum_j \frac{\gamma_j^2}{2|\varepsilon|^2}(\hat{n}_j^{(a)} + \hat{n}_j^{(b)}) \right] : \right\rangle, \qquad (11)$$

where, in accordance with equation (1), the difference photon number operator is $\hat{\Delta}_j = \hat{n}_j^{(a)} - \hat{n}_j^{(b)}$.

Ultimately, to evaluate equation (11) we need to express the spectral mode photon number operators, $\hat{n}_j^{(\mathrm{a})}$ and $\hat{n}_j^{(\mathrm{b})}$, in terms of the annihilation and creation operators associated with the temporal modes of the signal and LO. The spectral mode photon number operators are given by

$$\hat{n}_j^{(\mathrm{a})} = a_j^{\dagger(\mathrm{a})} a_j^{(\mathrm{a})} \qquad \text{and} \qquad \hat{n}_j^{(\mathrm{b})} = a_j^{\dagger(\mathrm{b})} a_j^{(\mathrm{b})} \tag{12}$$

where $\hat{a}_j^{(\mathrm{a,b})}$ and $\hat{a}_j^{\dagger(\mathrm{a,b})}$ are the annihilation and creation operators associated with the fields at the output ports of the apparatus. In terms of the signal and LO, the output port spectral mode annihilation and creation operators are given by

$$\hat{a}_j^{(\mathrm{a})} = r\hat{a}_j^{(\mathrm{s})} + t'\hat{a}_j^{(\mathrm{LO})} \qquad \text{and} \qquad \hat{a}_j^{(\mathrm{b})} = t\hat{a}_j^{(\mathrm{s})} + r'\hat{a}_j^{(\mathrm{LO})}, \tag{13}$$

where unitarity of the transformation requires that the complex transmission and reflection coefficients satisfy $rt' + tr'^{*} = 0$ [22]. We assume that $|t| = |r| = |t'| = |r'| = 1/\sqrt{2}$ for all wavelengths under consideration. That is, we assume the beamsplitter is 50 : 50, lossless, and broadband. Combining equations (13), and the corresponding relations for the creation operators, with equation (12), returns the ouput spectral mode photon number operators in terms of the signal and LO spectral mode annihilation and creation operators,

$$\hat{n}_j^{(\mathrm{a})} = \tfrac{1}{2}(\hat{n}_j^{(\mathrm{s})} + \hat{n}_j^{(\mathrm{LO})} + \hat{a}_j^{\dagger(\mathrm{s})}\hat{a}_j^{(\mathrm{LO})} + \hat{a}_j^{\dagger(\mathrm{LO})}\hat{a}_j^{(\mathrm{s})}), \tag{14}$$

and

$$\hat{n}_j^{(\mathrm{b})} = \tfrac{1}{2}(\hat{n}_j^{(\mathrm{s})} + \hat{n}_j^{(\mathrm{LO})} - \hat{a}_j^{\dagger(\mathrm{s})}\hat{a}_j^{(\mathrm{LO})} - \hat{a}_j^{\dagger(\mathrm{LO})}\hat{a}_j^{(\mathrm{s})}), \tag{15}$$

where, for simplicity, we have absorbed the phase shifts due to the beamsplitter into the definition of the LO annihilation and creation operators. Again, to evaluate $C_{\bar{\Delta}}(\{\gamma_j\})$ (see equation (11)) we must express $\hat{n}_j^{(\mathrm{a})}$ and $\hat{n}_j^{(\mathrm{b})}$ in terms of the temporal mode annihilation and creation operators associated with the signal and LO fields.

The resolution of the spectrometers and detector arrays is adequate for resolving the spectral beating between the LO ($k = 0$) and all of the temporal modes occupied by the signal ($0 \leqslant k \leqslant (N-1)$) and vacuum ($-(N-1) \leqslant k \leqslant 0$). Consequently, all $2N-1$ temporal modes contribute to the recorded photon numbers. Therefore, we express the spectral mode annihilation and creation operators as superpositions of the $2N-1$ temporal mode annihilation and creation operators, $\hat{b}_k$ and $\hat{b}_k^{\dagger}$ [23]. For instance, in terms of the temporal modes, the jth spectral mode annihilation operator is

$$\hat{a}_j = \frac{1}{N}\sum_{k=-(N-1)}^{(N-1)} \hat{b}_k \mathrm{e}^{\mathrm{i}2\pi jk/N}, \tag{16}$$

where the appropriate phase terms follow from the spectrometer resolution and corresponding definitions of ν_j and t_k, i.e. $\exp[\mathrm{i}2\pi\nu_j t_k] = \exp[\mathrm{i}2\pi jk/N]$. With the aid of equation (16), and the corresponding expression for the creation operators, we can now express the spectral mode photon number operators of equations (14) and (15) in terms of the temporal mode annihilation and creation operators,

$$\hat{n}_j^{(\mathrm{a})} = \frac{1}{2N}\sum_{k'}\sum_{k''} \mathrm{e}^{-\mathrm{i}2\pi j(k'-k'')/N} \times \{b_{k'}^{\dagger(\mathrm{LO})}\hat{b}_{k''}^{(\mathrm{LO})} + \hat{b}_{k'}^{\dagger(\mathrm{s})}\hat{b}_{k''}^{(\mathrm{s})} + \hat{b}_{k'}^{\dagger(\mathrm{s})}\hat{b}_{k''}^{(\mathrm{LO})} + \hat{b}_{k'}^{\dagger(\mathrm{LO})}\hat{b}_{k''}^{(\mathrm{s})}\}, \tag{17}$$

and

$$\hat{n}_j^{(\mathrm{b})} = \frac{1}{2N}\sum_{k'}\sum_{k''} \mathrm{e}^{-\mathrm{i}2\pi j(k'-k'')/N} \times \{b_{k'}^{\dagger(\mathrm{LO})}\hat{b}_{k''}^{(\mathrm{LO})} + \hat{b}_{k'}^{\dagger(\mathrm{s})}\hat{b}_{k''}^{(\mathrm{s})} - \hat{b}_{k'}^{\dagger(\mathrm{s})}\hat{b}_{k''}^{(\mathrm{LO})} - \hat{b}_{k'}^{\dagger(\mathrm{LO})}\hat{b}_{k''}^{(\mathrm{s})}\}. \tag{18}$$

Using equations (17) and (18) in equation (11) we find the desired expression for $C_{\bar{\Delta}}(\{\gamma_j\})$,

$$\begin{aligned} C_{\bar{\Delta}}(\{\gamma_j\}) &= (2|\varepsilon|)^{-N} \times \Bigg\langle : \exp\Bigg[\frac{-\mathrm{i}}{N|\varepsilon|}\sum_j \gamma_j \sum_{k'}\sum_{k''} \mathrm{e}^{-\mathrm{i}2\pi j(k'-k'')/N} \\ &\quad \times \{\hat{b}_{k'}^{\dagger(\mathrm{s})}\hat{b}_{k''}^{(\mathrm{LO})} + \hat{b}_{k'}^{\dagger(\mathrm{LO})}\hat{b}_{k''}^{(\mathrm{s})}\}\Bigg] \\ &\quad \times \exp\Bigg[-\sum_j \frac{\gamma_j^2}{2N|\varepsilon|^2}\sum_{k'}\sum_{k''} \mathrm{e}^{-\mathrm{i}2\pi j(k'-k'')/N} \\ &\quad \times \{\hat{b}_{k'}^{\dagger(\mathrm{LO})}\hat{b}_{k''}^{(\mathrm{LO})} + \hat{b}_{k'}^{\dagger(\mathrm{s})}\hat{b}_{k''}^{(\mathrm{s})}\}\Bigg] : \Bigg\rangle. \end{aligned} \tag{19}$$

To calculate the normally ordered quantum ensemble average of equation (19), we envoke the optical equivalence theorem [24, 25] and let $\hat{b} \to \beta$ and $\hat{b}^{\dagger} \to \beta^{*}$. The quantum ensemble average is then evaluated as a classical average with respect to the quasi-probability P distribution $\phi(\{\beta_{k'}^{(\mathrm{s})}\}, \{\beta_{k''}^{(\mathrm{LO})}\})$. For the coherent, single temporal mode ($k = 0$) LO and the unknown multitemporal mode signal field considered here, the P distribution is

$$\phi(\{\beta_{k'}^{(\mathrm{s})}\}, \{\beta_{k''}^{(\mathrm{LO})}\}) = \phi(\{\beta_{k'}^{(\mathrm{s})}\})\delta^2(\beta_{k''=0}^{(\mathrm{LO})} - \varepsilon)\prod_{k''\neq 0}\delta^2(\beta_{k''}^{(\mathrm{LO})}). \tag{20}$$

Thus, the scaled difference count characteristic function is

$$\begin{aligned} C_{\bar{\Delta}}(\{\gamma_j\}) &= (|\varepsilon|)^{-N}\iint \mathrm{d}^2\{\beta_{k'}^{(\mathrm{s})}\}\,\mathrm{d}^2\{\beta_{k''}^{(\mathrm{LO})}\} \\ &\quad \times \left\{\begin{array}{l} \phi(\{\beta_{k'}^{(\mathrm{s})}\})\delta^2(\beta_{k''=0}^{(\mathrm{LO})} - \varepsilon)\prod_{k''\neq 0}\delta^2(\beta_{k''}^{(\mathrm{LO})}) \\ \times \exp\Big[\frac{-\mathrm{i}}{N|\varepsilon|}\sum_j \gamma_j \sum_{k'}\sum_{k''} \mathrm{e}^{-\mathrm{i}2\pi j(k'-k'')/N} \\ \qquad \times \{\beta_{k'}^{*(\mathrm{s})}\beta_{k''}^{(\mathrm{LO})} + \mathrm{e}^{\mathrm{i}\theta} + \beta_{k'}^{*(\mathrm{LO})}\beta_{k''}^{(\mathrm{s})}\mathrm{e}^{-\mathrm{i}\theta}\}\Big] \\ \times \exp\Big[-\sum_j \frac{\gamma_j^2}{2N|\varepsilon|^2}\sum_{k'}\sum_{k''} \mathrm{e}^{-\mathrm{i}2\pi j(k'-k'')/N} \\ \qquad \times \{\beta_{k'}^{*(\mathrm{LO})}\beta_{k''}^{(\mathrm{LO})} + \beta_{k'}^{*(\mathrm{s})}\beta_{k''}^{(\mathrm{s})}\}\Big] \end{array}\right\} \end{aligned} \tag{21}$$

where θ is the phase of the LO relative to the signal, including the phase contribution of the beamsplitter. Upon performing the integration over $\mathrm{d}^2\{\beta_{k''}^{(\mathrm{LO})}\}$, and setting all of the $\beta_{k'}^{*(\mathrm{s})}\beta_{k''}^{(\mathrm{s})}/|\varepsilon|^2$ terms equal to zero, since the LO is much stronger than the signal, equation (21) simplifies to

$$\begin{aligned} C_{\bar{\Delta}}(\{\gamma_j\}) &= (|\varepsilon|)^{-N}\exp\Bigg[-\sum_j \frac{\gamma_j^2}{2N}\Bigg]\int \mathrm{d}^2\{\beta_{k'}^{(\mathrm{s})}\}\phi(\{\beta_{k'}^{(\mathrm{s})}\}) \\ &\quad \times\exp\Bigg[\frac{-\mathrm{i}}{N}\sum_j \gamma_j \sum_{k'}\{\mathrm{e}^{-\mathrm{i}2\pi jk'/N}\beta_{k'}^{*(\mathrm{s})}\mathrm{e}^{\mathrm{i}\theta} + \mathrm{e}^{\mathrm{i}2\pi jk'/N}\beta_{k'}^{(\mathrm{s})}\mathrm{e}^{-\mathrm{i}\theta}\}\Bigg]. \end{aligned} \tag{22}$$

Recall that the apparatus and inversion routine returns the joint probability, $P_{\kappa}(\{\kappa_k\})$, for measuring the set, $\{\kappa_k\}$,

of Fourier transformed difference counts. Consequently, we need to determine the associated characteristic function $C_\kappa(\{\xi_k\})$. Following the prescription given in equation (5), we obtain the scaled characteristic function $C_{\bar{k}}(\{\xi_k\})$ by setting $\gamma_j = \sum_k (\xi_k \exp[-\mathrm{i}2\pi jk/N] + \xi_k^* \exp[\mathrm{i}2\pi jk/N])$ in equation (22):

$$C_{\bar{\kappa}}(\{\xi_k\}) = (|\varepsilon|)^{-N} \int \mathrm{d}^2\{\beta_{k'}^{(\mathrm{s})}\}\phi(\{\beta_{k'}^{(\mathrm{s})}\}) \times \left\{ \begin{array}{l} \exp\left[\frac{-\mathrm{i}}{N}\sum_{j,k,k'}\left[\begin{array}{l}(\xi_k \mathrm{e}^{-\mathrm{i}2\pi jk/N} + \xi_k^* \mathrm{e}^{\mathrm{i}2\pi jk/N}) \\ \times(\mathrm{e}^{-\mathrm{i}2\pi jk'/N}\beta_{k'}^{*(\mathrm{s})}\mathrm{e}^{\mathrm{i}\theta} + \mathrm{e}^{\mathrm{i}2\pi jk'/N}\beta_{k'}^{(\mathrm{s})}\mathrm{e}^{-\mathrm{i}\theta})\end{array}\right]\right] \\ \times\exp\left[-\frac{1}{2N}\sum_{j,k,k'}\left[\begin{array}{l}(\xi_k \mathrm{e}^{-\mathrm{i}2\pi jk/N} + \xi_k^* \mathrm{e}^{\mathrm{i}2\pi jk/N}) \\ \times(\xi_{k'}\mathrm{e}^{-\mathrm{i}2\pi jk'/N} + \xi_{k'}^*\mathrm{e}^{\mathrm{i}2\pi jk'/N})\end{array}\right]\right] \end{array} \right\}. \tag{23}$$

The summations over j return Kronecker delta functions. Summation over k' simplifies equation (23) to

$$C_{\bar{\kappa}}(\{\xi_k\}) = (|\varepsilon|)^{-N} \int \mathrm{d}^2\{\beta_{k'}^{(\mathrm{s})}\}\phi(\{\beta_{k'}^{(\mathrm{s})}\}) \times \left\{ \begin{array}{l} \exp\left[-\mathrm{i}\sum_k \left[\begin{array}{l}\xi_k\beta_{-k}^{*(\mathrm{s})}\mathrm{e}^{\mathrm{i}\theta} + \xi_k\beta_{+k}^{(\mathrm{s})}\mathrm{e}^{-\mathrm{i}\theta} \\ +\xi_k^*\beta_{+k}^{*(\mathrm{s})}\mathrm{e}^{\mathrm{i}\theta} + \xi_k^*\beta_{-k}^{(\mathrm{s})}\mathrm{e}^{-\mathrm{i}\theta}\end{array}\right]\right] \\ \times\exp\left[-\frac{1}{2}\sum_k\left[\xi_{-k}\xi_k + \xi_{-k}^*\xi_k^* + 2|\xi_k|^2\right]\right] \end{array} \right\}. \tag{24}$$

Equation (24) is the characteristic function associated with the probability distribution, $P_\kappa(\{|\varepsilon|\kappa_k\}) \equiv P_{\bar{\kappa}}(\{\bar{\kappa}_k\})$, for measuring the set of scaled Fourier transformed difference counts for all k, $-(N-1) \leqslant k \leqslant (N-1)$. But, as we noted in section 2, since the difference count data are real, the complex Fourier transform variables satisfy $\kappa_{-k} = \kappa_k^*$. Since we are only interested in the reduced range $1 \leqslant k \leqslant (N-1)$, we set $\xi_k = 0$ for all $-(N-1) \leqslant k \leqslant 0$ (this is formally equivalent to projecting the $2N-1$ complex variable probability distribution into the desired $N-1$ complex variable space). Moreover, since all the modes preceding the LO are in the vacuum state, $\beta_{-k}^{(\mathrm{s})} = 0$. Hence, for the temporal modes of interest, the characteristic function associated with the scaled Fourier transformed difference counts is

$$C_{\bar{\kappa}}(\{\xi_k\}) = (|\varepsilon|)^{-N}\exp\left[-\sum_{k=1}^{(N-1)}|\xi_k|^2\right]\int \mathrm{d}^2\{\beta_{k'}^{(\mathrm{s})}\}\phi(\{\beta_{k'}^{(\mathrm{s})}\}) \times\left\{\exp\left[-\mathrm{i}\sum_{k=1}^{(N-1)}(\xi_k\beta_k^{(\mathrm{s})}\mathrm{e}^{-\mathrm{i}\theta} + \xi_k^*\beta_k^{*(\mathrm{s})}\mathrm{e}^{\mathrm{i}\theta})\right]\right\}. \tag{25}$$

$C_{\bar{k}}(\{\xi_k\})$ is proportional to the characteristic function associated with the $N-1$ temporal mode Q-function, $Q(\{\beta_k\})$, describing the joint quantum statistics of the signal field [20, 26]. Consequently,

$$P_{\bar{\kappa}}(\{\bar{\kappa}_k\}) = P_\kappa(\{\varepsilon\kappa_k\}) = Q(\{\beta_k\}). \tag{26}$$

4. Simulation: the two-time correlation function

The MTHD apparatus and inversion routine returns the $N-1$ temporal-mode Q-function, $Q(\{\beta_k\})$, describing the joint quantum statistics of the signal field. Of course, to reconstruct the Q-function with adequate dynamic range for evaluating coherences between large numbers of temporal modes requires the collection of a relatively large amount of data. But lower-order coherences, such as the normalized two-time correlation function (second-order coherence),

$$g^{(2)}(t_k, t_{k'}) = \langle \hat{b}_k^\dagger \hat{b}_{k'}^\dagger \hat{b}_k \hat{b}_{k'}\rangle / \langle \hat{b}_k^\dagger \hat{b}_k\rangle\langle \hat{b}_{k'}^\dagger \hat{b}_{k'}\rangle, \tag{27}$$

provide a measure of the state of a quantum field without requiring the collection of a large amount of data. The second-order coherence is a particularly useful quantity since it can distinguish between classical (e.g. photon-bunched [27]) and nonclassical (e.g. photon-antibunched [28]) states of the field. In this section, we evaluate simulated MTHD data of chaotic, thermal-like light and show that $g^{(2)}(t_k, t_{k'})$ is reliably reconstructed from a minimal amount of MTHD data.

The second-order coherence of equation (27) is readily evaluated from knowledge of $Q(\{\beta_k\})$. The quantum expectation of any operator of the form $\hat{O}^a(\{\hat{b}_k\}\{b_k^\dagger\})$ with the temporal mode annihilation and creation operators arranged in antinormal order can be evaluated as a quasi-classical average over $Q(\{\beta_k\})$ [26, 29]. The procedure is straightforward: first, construct $Q^a(\{\beta_k\})$ from $\hat{O}^a(\{\hat{b}_k\}\{b_k^\dagger\})$

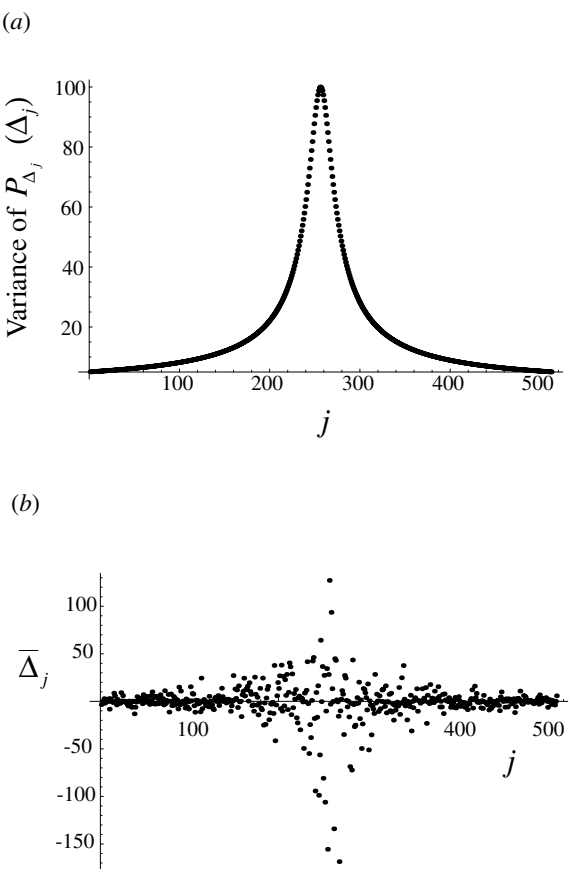

Figure 2. (*a*) The variance of the Gaussian distributions, $P_{\Delta_j}(\Delta_j)$, describing the probability of measuring the difference photon numbers, Δ_j, for chaotic light. For this example, the mean number of photons follows a Lorentzian distribution in frequency (j). (*b*) A representative example of the simulated difference photon number data.

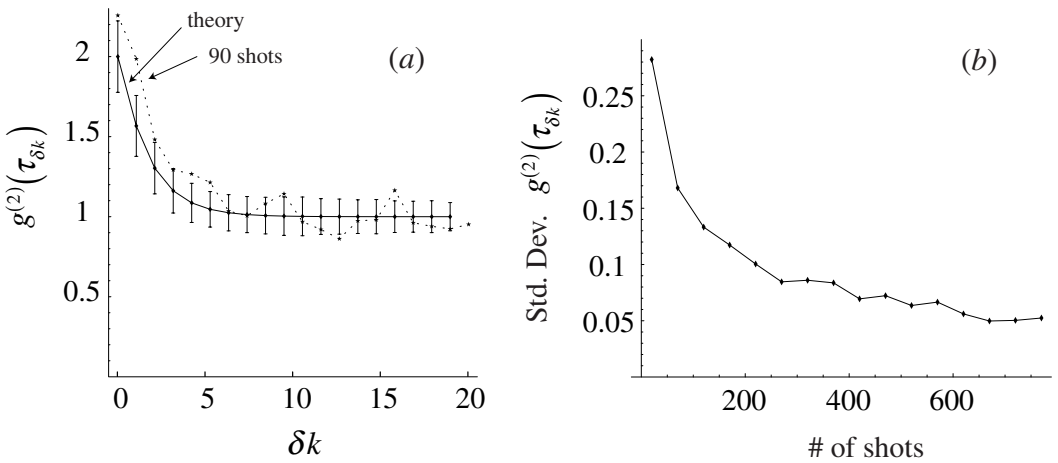

Figure 3. (*a*) The second-order coherence for the simulated example of chaotic light. The full curve is theory, and the dotted curve is the MTHD reconstruction after only 90 shots. The error bars indicate the standard deviation of 2000 realizations of the 90-shot reconstruction. (*b*) The standard deviation of the second-order coherence at $\delta k = 1$ as a function of the number of shots. The error decreases as the square root of the number of shots.

by setting $\hat{b}_k = \beta_k$ and $\hat{b}_k^\dagger = \beta_k^*$. Then the quantum expectation value, $\langle \hat{O}^a \rangle$, is simply

$$\langle \hat{O}^a(\{\hat{b}_k\}\{\hat{b}_k^\dagger\})\rangle = \langle O^a(\{\beta_k\})\rangle_c = \int \mathrm{d}^2\{\beta_k\} O^a(\{\beta_k\}) Q(\{\beta_k\}). \tag{28}$$

To evaluate $g^{(2)}(t_k, t_{k'})$, we arrange the operators in antinormal order by using the commutation relation $[\hat{b}_k, \hat{b}_{k'}^\dagger] = \delta_{k,k'}$ [23], and following the prescription of equation (28). In terms of the quasi-classical averages, the second-order coherence is

$$g^{(2)}(t_k, t_{k'}) = \frac{\langle \beta_k \beta_{k'} \beta_k^* \beta_{k'}^* - \beta_k \beta_k^* - \beta_{k'} \beta_{k'}^* - 1\rangle_c}{\langle \beta_k \beta_k^* - 1\rangle \langle \beta_{k'} \beta_{k'}^* - 1\rangle_c}. \tag{29}$$

The multimode Q-function required to evaluate equation (29), is built up in a shot-to-shot fashion from the measured sets of spectral mode difference photon numbers $\{\Delta_j\}$. For chaotic light, the probability of measuring the set of difference counts factorizes into a product of probabilities for measuring the difference photon number at every frequency, $P_\Delta(\{\Delta_j\}) = \Pi_j P_{\Delta j}(\Delta_j)$. Each individual spectral mode difference photon number probability distribution, $P_{\Delta j}(\Delta_j)$, is a Gaussian whose variance is a function of the mean number of signal photons [30]. For this example, the mean number of signal photons is a Lorentzian distribution in frequency with a peak of 10 000 photons. Figure 2(*a*) shows the variance of the individual probability distributions for the chosen Lorentzian line shape.

We use $P_\Delta(\{\Delta_j\})$ to simulate difference photon number data. Figure 2(*b*) is a representative example of simulated data for a single shot of the experiment. Each shot contributes one point to the $N-1$ mode Q-function. For chaotic light, the second-order coherence depends solely on the time difference, $\tau_{\delta k} = t_{k'} - t_k$ [31]. With the aid of equation (29), we calculate $g^{(2)}(\tau_{\delta k})$ from the reconstructed Q-function. Figure 3(*a*) shows the results of the simulation. The dotted curve is $g^{(2)}(\tau_{\delta k})$ calculated after 90 shots. The full curve, which lies on top of the theory to within an error of a quarter of a per cent, is the mean of 2000 90-shot reconstructions of $g^{(2)}(\tau_{\delta k})$. The error bars show the standard deviation associated with the 90-shot subsets. After only 90 shots, the reconstruction is accurate to within $\pm 12\%$. As illustrated in figure 3(*b*), the reconstruction improves as the number of shots is increased. Not surprisingly, the error decreases as the square root of the total number of shots. A total of 16 000 shots returns a reconstruction error of less than $\pm 1\%$. At a repetition rate of 10 Hz, such an experiment would require less than 30 min to collect the necessary data.

5. Conclusions

In this paper we proposed a novel method for measuring the multitemporal mode statistics of repetitive quantum fields. The technique, multitemporal mode heterodyne detection (MTHD), combines a strong coherent state LO and a weak quantum signal on a beamsplitter. The LO occupies a single temporal mode while the signal may occupy multiple temporal modes. The signal lags the LO and consequently their two spectra interfere. At both output ports of the beamsplitter the interference is resolved by a spectrometer, and the number of photons per spectral mode is recorded by a linear detector array. On each shot of the experiment, a multichannel differencer determines the set of spectral mode difference photon numbers between the combined fields at the two output ports of the beamsplitter. A quantum-mechanical analysis reveals that the probability for obtaining the Fourier transformed difference counts is proportional to the multitemporal mode Q-function describing the joint quantum statistics of the signal field.

Since any antinormally ordered combination of the temporal mode annihilation and creation operators can be calculated from knowledge of the multitemporal mode Q-function, the MTHD device can be used to measure quantum correlations between temporal modes. As an example, we calculated the second-order coherence of chaotic light from simulated MTHD data. The simulation reveals that only a minimal amount of data is required to accurately reconstruct the two-time correlations. Of course, since the MTHD

apparatus measures all of the temporal modes simultaneously, it should provide an efficient method of characterizing fields that may exhibit multimode correlations, such as squeezed solitons [32], or fields generated by noninstantaneous nonlinear interactions like impulsive stimulated Raman scattering.

References

[1] Yuen H P and Chan V W S 1983 *Opt. Lett.* **8** 177
[2] Abbas G L, Chan V W S and Yee T K 1983 *Opt. Lett.* **8** 419
[3] Walker N G and Carroll J E 1986 *Opt. Quantum Electron.* **18** 355
[4] Shapiro J H and Wagner S S 1984 *IEEE J. Quantum Electron.* **20** 803
[5] Smithey D T, Beck M, Raymer M G and Faridani A 1993 *Phys. Rev. Lett.* **70** 1244
[6] Vogel K and Risken H 1989 *Phys. Rev.* A **40** 2847
[7] D'Ariano G M, Macchiavello C and Paris M B A 1994 *Phys. Rev.* A **50** 4298
[8] Kuhn H, Welsch D G and Vogel W 1994 *J. Mod. Opt.* **41** 1607
[9] Leonhardt U, Munroe M, Kiss T, Richter Th and Raymer M G 1996 *Opt. Commun.* **127** 144
[10] Anderson M E, Beck M, Raymer M G and Bierlein J D 1995 *Opt. Lett.* **20** 620
[11] Raymer M G, Cooper J, Carmichael H J, Beck M and Smithey D T 1995 *J. Opt. Soc. Am.* B **12** 1801
[12] Raymer M G, McAlister D F and Leonhardt U 1996 *Phys. Rev.* A **54** 2397
[13] Opatrny T, Welsch D G and Vogel W 1997 *Phys. Rev.* A **55** 1416
[14] McAlister D F and Raymer M G 1997 *Phys. Rev.* A **55** 1609
[15] Vasilyev M, Choi S-K, Kumar P and D'Ariano G M 2000 *Phys. Rev. Lett.* **84** 2354
[16] Raymer M G and Funk A C 2000 *Phys. Rev.* A **61** 015 801
[17] D'Ariano G M, Sacchi M F and Kumar P 2000 *Phys. Rev.* A **61** 013 806
[18] Raymer M G, Cooper J and Beck M 1993 *Phys. Rev.* A **48** 4617
[19] Yuen H P and Shapiro J H 1980 *IEEE Trans. Info. Theor.* **26** 78
[20] Vogel W and Welsch D G 1995 *Acta Phys. Slovaca* **45** 313
[21] Walker N G 1987 *J. Mod. Opt.* **34** 15
[22] Ou Z Y, Hong C K and Mandel L 1997 *Opt. Commun.* **63** 118
[23] Titulaer U M and Glauber R J 1966 *Phys. Rev.* **145** 1041
[24] Glauber R J 1963 *Phys. Rev. Lett.* **10** 84
[25] Sudarshan E C G 1963 *Phys. Rev. Lett.* **10** 277
[26] Cahill K E and Glauber R J 1969 *Phys. Rev.* **177** 1882
[27] Hanbury Brown R and Twiss R Q 1956 *Nature (London)* **177** 27
[28] Kimble H J, Dagenais M and Mandel L 1977 *Phys. Rev. Lett.* **39** 691
[29] Hillery M, O'connell R F, Scully M O and Wigner E P 1984 *Phys. Rep.* **106** 121
[30] Leonhardt U 1997 *Measuring the Quantum State of Light* (Oxford: Oxford University Press)
[31] Loudon R 1983 *The Quantum Theory of Light* 3rd edn (Oxford: Oxford University Press)
[32] Spalter S, Korolkova N, Konig F, Sizmann A and Leuchs G 1998 *Phys. Rev. Lett.* **81** 786